Flood Hazard Mapping and Monitoring in the Kamrup District of the Lower Brahmaputra Valley, Assam: A Geospatial Appraisal

Biswajit Bordoloi, Krishna Bora, Sahil Choudhury, Kongkona Sonowal, Sunayana Sahu, Debika Hazarika, and Pranamika Deka

Abstract Floods are one of the most cataclysmic events occurring globally. Amongst the South Asian nations, India is one of the most highly flood-prone countries. More than 40 million hectares are flood-vulnerable out of the total geographical area of 329 million hectares. The months of June to September receive an over 80% precipitation in the country. The state of Assam, bearing a vast network of rivers and more than 50 tributaries of Brahmaputra and Barak surpasses through flood catastrophe annually. The flood-prone area of the state as assessed by the Rashtriya Barh Ayog (RBA) is 31.05 lakh hectares against the total area of the state of 78.523 lakh hectares i.e., about 39.58% of the total land area of Assam (Flood and Erosion Problems 2023). Such a loss calls for an effective management strategy, amongst which Geoinformatics plays a vital role. Being an umbrella science, it examines and assists evaluators in managing a hazard effectively to a great extent. Hence, the study of flood hazards through the lens of geoinformatics becomes crucial. This chapter attempts to appraise the role of geoinformatics in the flood-affected district of Kamrup, Assam. The Analytical Hierarchy Process (AHP) method has prepared the flood hazard map. During flood disasters, remote sensing and GIS technologies can monitor the situation and give decision-makers geographically dispersed statistics for prompt preparation, recovery, and mitigation plans. Thus, this study provides

B. Bordoloi (✉) · S. Choudhury
Department of Geography, Pandu College, Guwahati, Assam, India
e-mail: bordoloibiswajit38@gmail.com

S. Choudhury
e-mail: choudhurysahil68@panducollege.ac.in

K. Bora
Athkhelia Jatiya Vidyalaya, Golaghat, Assam, India

K. Sonowal
Department of Geography, Dudhnoi College, Goalpara, Assam, India

S. Sahu · D. Hazarika · P. Deka
Independent Researcher, Guwahati, Assam, India

© The Author(s), under exclusive license to Springer Nature Singapore Pte Ltd. 2024

B. Biswas and B. B. Ghute (eds.), *Flood Risk Management*, Springer Natural Hazards,
https://doi.org/10.1007/978-981-97-2688-2_18

an innovative view of flood hazard mapping and remarkably contributes to flood monitoring.

Keywords Brahmaputra · Flood · Hazard · Preparedness · Remote sensing and GIS · AHP

1 Introduction

The Earth undergoes dynamic changes due to the continuous interplay of both internal and external forces acting upon it. These changes disturb the overall equilibrium of the planet. Consequently, the occurrence of hazards becomes visible. Human activities further wind up these changes, which are responsible for increasing the intensity and frequency of these hazards.

By definition, a natural hazard is an occurrence or a phenomenon that results from physical forces and circumstances that happen on the surface of the Earth. This occurrence is referred to as a hazardous event when it occurs in a crowded region. Although "hazard" and "disaster" are used interchangeably, they differ significantly. When a hazard has an impact on a population, a disaster occurs. It is summarized as a dangerous occurrence that seriously harms the environment, livelihood patterns, property, and the human population. Flood is a hazard caused by rising water in an existing waterway, such as a river or drainage. Centre for Research on the Epidemiology of Disasters (CRED) has defined flood as "being a state of the rise of water level in coastal areas, lakes, streams, and channels" (Rehman et al. 2019). The UN Office for Disaster Risk Reduction (UNISDR) and the Centre for Research on Epidemiology of Disasters (CRED) produced research stating that floods caused US$656 billion in economic damage worldwide between 1998 and 2017 (Anusha 2021). By 2050, annual economic causalities caused by floods globally may exceed US$1 trillion (Anusha 2021). According to UNISDR and CRED reports, about 142,088 people lost their lives, and more than 2 billion people are likely to have been affected or grieved around the world due to floods between the years 1998 and 2017 (Anusha 2021).

Flood threats have impacted many individuals in the years 1980, 1993, 2002, and 2004. Approximately 2.3 billion individuals, or 56% of the world's population, were impacted by floods between 1995 and 2015. Between 2005 and 2015, flood dangers impacted almost 560,000 persons in South America alone. Flood hazards wreaked havoc on the environment and the lives of people in the least developed countries, causing severe damage to infrastructure and putting lives and economic prosperity at risk. During the past decade, it has resulted in disastrous situations and significant losses in terms of lives and property in countries including Bangladesh, Mozambique, Germany, India, China, and the United States (Rehman et al. 2019).

With a rising tendency of natural and man-made hazards, research on disaster-related issues and their level of study is gaining traction in the Indian setting. The Disaster Management Act, 2005, which the Indian government passed, is one clear

example of it. (Hazarika 2015). This Act is what makes catastrophe management a serious, cross-cutting topic combined with a developmental strategy. The Act has maintained a bottom-up approach by advocating for different process stakeholders to play specific roles at different levels. (Hazarika 2015). To address the issue of disaster management at the grassroots level and foster mutual knowledge for its resolution, this act establishes three tier agencies under the government mechanism: the National Disaster Management Authority (NDMA), State Disaster Management Authority (SDMA), and District Disaster Management Authority (DDMA) (Hazarika 2015).

Some of the devastating floods witnessed in India are the 2008 Kosi floods in north Bihar, the 2010 Leh, Jammu & Kashmir flash floods (Bhatt and Rao 2014), the 2010 Ganga River floods, the 2012 Assam floods, the floods in the year 2013 in Uttarakhand, the year 2014 in Jammu and Kashmir, the year 2017 in the Rapti River basin, and the year 2018 in Kerala (Anusha 2021).

The river banks of Brahmaputra and Barak get flooded due to the surplus water found in the Brahmaputra and Barak basins (Manual for Data Collection in Census of Water Bodies n.d.). Excess water flow ruptures Brahmaputra's banks and causes floods in Assam. Arunachal Pradesh, Nagaland and Manipur. The Brahmaputra flood of 2016 was the last major flood that caused widespread destruction in Assam. Arunachal Pradesh, Manipur, and Nagaland.

Flood maps are a vital tool for providing valuable information for reducing flood damage and spatial planning purposes (Tam et al. 2013). The geospatial techniques provide a framework for the identification of submerged areas. Remote sensing imagery is a vital tool for charting the area flooded under floodwaters following an event. This chapter takes a geographical approach to investigating the potentially dangerous role of floods in Assam's Brahmaputra Valley. Although the valley covers a larger area, Kamrup district has been chosen for the current chapter while considering several limitations, including time and data availability.

2 Rationalization of the Study Area

Kamrup is situated on the north and south bank plain of the mighty Brahmaputra River of Assam. It extends between 25.46°N to 26.49°N latitude and 90.48°E to 91.50°E longitude (Fig. 1). The total geographical area is 3,084.14 square km. Except for the small hilly tracts of the southern Kamrup belt, almost the entire district is plain, including a few parcels of land on the bank of Brahmaputra (Lahkar 2017). The total population of the district is 1,517,202 people. There are 139 gaon panchayats and 14 blocks, which are inhabited by both tribal and non-tribal communities. The fifth largest rural population among the districts of Assam resides here, in number it is 1375148, of which males and females are 706,140 and 669,008, respectively. The population density per square km is 489 (as per the 2011 census). The alluvial plain mostly covers the district, mainly formed by the mighty Brahmaputra and its tributaries. The plain is made up of both new and old alluvium. The study area experiences a humid sub-tropical climate with the impact of monsoons during the

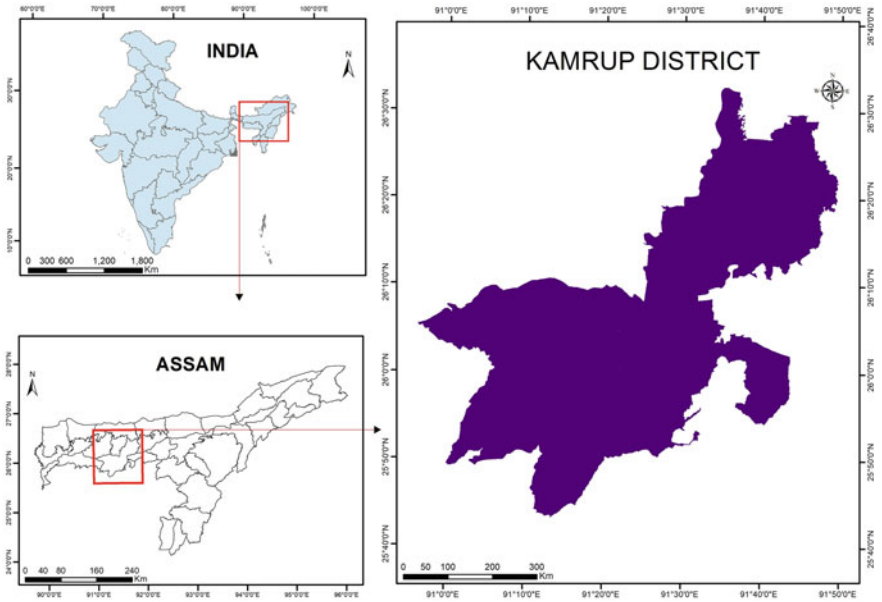

Fig. 1 Location map of study area

summer season. The average temperature during summer is 32 °C, and during the winter is 17 °C. The district enjoys a cool and dry winter and rainy summer. The monsoon wind system mainly determines the climate of Kamrup district. The study area receives rainfall from late April to late September; temperature is also relatively higher in these months. Winter is most prominent in December and January. The major soil types found in Kamrup district are alluvial soil, red soil, and laterite soil. The main soil type of the district varies from sandy loam, loam, sandy clay, and clay loam.

3 Database and Methodology

The current chapter incorporates both primary and secondary datasets into a GIS interface. A detailed data description has been provided in the table (Table 1). The research area's flood risk zones were determined using a multi-parametric dataset. Twelve influencing layers have been considered while preparing the flood risk map of Kamrup district. The twelve layers included maps of slope, land use and land cover (LULC), geology, geomorphology, soil, rainfall, and elevation, as well as the topographic wetness index (TWI), stream power index (SPI), sediment transport index (STI), and topographic roughness index (TRI).

Table 1 Data description

Data type	Description	Source
Digital elevation model (DEM) data	Shuttle radar topography mission (SRTM 1 arc-second global) (30 m resolution)	USGS Earth Explorer https://earthexplorer.usgs.gov
Satellite imagery	Sentinel-2A (10 m resolution)	Copernicus Open Access Hub https://scihub.copernicus.eu (accessed on January 1st, 2023)
Soil data	Soil map of India	Food and Agriculture Organization of the United Nations https://www.fao.org/soils-portal/data-hub/soil-maps-and-databases/faounesco-soil-map-of-the-world/en/
Rainfall data	The average annual rainfall	CHRS Data Portal https://chrsdata.eng.uci.edu (From 2003 to 2020)
Geology and geomorphology data	Geology and geomorphology map of India	Bhukosh—Geological Survey of India https://bhukosh.gsi.gov.in

SRTM 1 Arc-Second Global (30 m resolution) DEM data was downloaded from USGS Earth Explorer. The data was used to prepare slope, elevation, TRI, TWI, SPI, STI, and distance from the river maps using ArcGIS 10.3.

Topographic Roughness Index (TRI), as defined, is the study basin's local topography (Amen et al. 2023). The topographic roughness index (TRI) is given as (Stambaugh and Guyette 2008):

$$\text{TRI} = \frac{Area_V - Area_I}{Area_P - Area_I}$$

where

Area_V (A_V) denotes the variable surface area
Area_P (A_P) denotes the planimetric surface area
Area_I (A_I) denotes the area of interest (Stambaugh and Guyette 2008).

Using the Topographic Wetness Index (TWI), one may determine which areas are flooded during floods and evaluate how topography affects a watershed's hydrological process (Gupta and Dixit 2021). It was formulated by Beven and Kirkby in 1979 (Gupta and Dixit 2021):

$$\text{TWI} = \ln\left(\frac{A}{\tan_\beta}\right)$$

where

'A' represents the source contributing area
'$\tan_\beta$' is the ground surface slope (Gupta and Dixit 2021).

The SPI regulates the potential erosive force of water flow and describes the possibility of flow erosion at the specified surface point (Bachri et al. 2019; Rehman et al. 2019)

$$\mathrm{SPI} = A_s \tan_\beta$$

where

'A_s' is the exact catchment area
'$_\beta$' is the slope gradient (radians) (Amen et al. 2023).

Another factor that contributes to flooding is the STI, which has the potential to increase the frequency of floods and damage foundations (Amen et al. 2023).

$$\mathrm{STI} = \left(\frac{A_s}{22.13}\right)^{0.6}\left(\frac{\sin_\beta}{0.0896}\right)^{1.3}$$

where

'A_s' is the upstream region
'$_\beta$' is the slope of each pixel (Amen et al. 2023).

The DEM data was used to calculate the distance (in meters) from the river. With ArcMap's hydrology and proximity tools, flow direction, flow accumulation, stream link, stream to feature, and multiple ring buffer layers are created for this fill.

To create the LULC map, Sentinel-2A satellite imagery with a 10 m spatial resolution was acquired from Copernicus Open Access Hub on January 1st, 2023. The soil map of the study area was prepared from the digitized version of the FAO-UNESCO DSMW (Digital Soil Map of the World) bearing a scale of 1:5,000,000 (Rehman et al. 2019; Rahimi et al. 2023). Further geology and geomorphology maps of Kamrup district were prepared from the data derived from GSI Bhukosh.

The Center for Hydrometeorology and Remote Sensing (CHRS) portal was used to gather historical rainfall data spanning the last 18 years (2003–2020). Data was extracted from the 4 km × 4 km resolution PERSIANN-CCS dataset. The rainfall data of the study area was extracted from eight rainfall stations, namely Hajo, Rangia, Chaygaon, Bezera, Boko, Goroimari, Sualkuchi, and Rani. The spatial distribution of the average annual rainfall of the research area was created using the Inverse Distance Weighted (IDW) approach. One of the earliest spatial prediction techniques for point data interpolation is inverse distance weighted (IDW). It uses a linearly weighted combination of sample points to calculate cell values. Weight (W = 1/dp) is a function of inverse distance (Choudhury and Garg 2021). The location-dependent variable's surface ought to be the one being interpolated. According to this approach, the variable being mapped has less of an impact the further it is from the sampled place (Choudhury and Garg 2021). IDW is an exact interpolation method where the position of the predicted value is determined by

$$Zp = \frac{\sum_{i=1}^{n}\left(\frac{Z_i}{d_i^p}\right)}{\sum_{i=1}^{n}\left(\frac{1}{d_i^p}\right)}$$

where

Z_p Predicted value
Z_i value at *i* measured point
d_i distance of i measured location to the predicted point
p power function
n number of points to be used (Choudhury and Garg 2021).

The significance of known points on the interpolated values based on their separation from the output point is controlled by the power value "p." It is a real, positive number, and its default value is always 2. A greater power value can be defined to emphasize the closest points more. The surface will, therefore, have more detail and be less smooth since adjacent data will have the greatest influence. With an increase in power, the interpolated values start to converge towards the value of the closest sample point. A smoother result will arise from specifying a lower value for power, which will give greater influence to surrounding points that are farther away (Choudhury and Garg 2021).

All the prepared maps were converted into the Projected Coordinate System (PCS) under UTM Zone 46°N. The flood risk influencing feature layers were resampled and reclassified in the ArcGIS interface. These reclassified maps were integrated using the Weighted Overlay tool of ArcGIS.

Overlay analysis in GIS is performed to superimpose the multiple layers of datasets that represent different themes together to identify the relationship of each layer. Overlay analysis represents the composite map by the combination of different attributes and geometries of datasets. In the overlay analysis, new spatial datasets are created by merging data from two or more input data layers (Reddy and Singh 2018; Choudhury and Garg 2021). To address multi-criteria issues like site selection and appropriateness models, the Weighted Overlay tool employs one of the most used overlay analysis techniques (Choudhury and Garg 2021). The technique has the advantage that human judgment can be integrated with this analysis (Choudhury and Garg 2021).

One of the best techniques for integration is the Analytical Hierarchy Process (AHP), which gives various weights to each flood-related element. The analytical hierarchy process is a flexible and organized method for deciphering multi-factor difficult decision scenarios (Amen et al. 2023). Twelve flood conditioning variables are employed, together with data from DEM, satellite imageries of the LULC map, rainfall data, soil, geology, and geomorphology to construct different layers. A flood hazard map is produced by superimposing the parameters in the ArcGIS interface according to weights that have been assigned. The weightage is generated in between 0 and 9 Saaty's fundamental scale. AHP served as a way to categorize various criteria within the criterion into various suitability levels (Sonowal and Choudhury 2023). Thomas L. Saaty based AHP on his experience and created it in 1977 (Sonowal and

Table 2 Saaty's scale of relative importance

Intensity of importance	Definition
1	Equal importance
3	Moderately importance
5	Strongly importance
7	Very strongly importance
9	Extremely importance
2, 4, 6, 8	Intermediate values

(*Source* Choudhury and Garg 2021)

Choudhury 2023). Saaty (Saaty 2008) established the consistency ratio (CR), which is the ratio of the random index (RI) to the consistency index (CI), to assess the consistency of the matrix (Sonowal and Choudhury 2023). If the consistency ratio (CR) is less than 0.1 (10%), it can be considered suitable for additional examination. The matrix's characteristics determine the RI, which is a fixed number (Sonowal and Choudhury 2023). The following formula ensures consistency (Amen et al. 2023):

$$\mathrm{CR} = \frac{CI}{RI} \quad \mathrm{CI} = \frac{\lambda_{\max} - n}{n - 1} \text{ (Amen et al. 2023)}$$

where, n is the number of components, λ_{max} is the matrix's Principal Eigenvalue, CI is the consistency index, RI is the random index, and CR stands for consistency ratio (Amen et al. 2023). The primary Eigenvalue is obtained by multiplying each element of the Eigenvector by the total number of columns of the reciprocal matrix (Sonowal and Choudhury 2023). Table 2 shows Saaty's fundamental scale of relative importance, based on which the pairwise comparison matrix was developed (Table 3) on the AHP Template (Choudhury and Garg 2021). In this chapter, the percentage of weight is generated using a pairwise comparison matrix table ranging the class 1–5 (very low to very high) based on the significance of each class of each flood causative criterion (Fig. 2).

4 Results and Discussion

The possible zones for flood risk and vulnerability depend on analyzing different parameters such as slope, Topographic wetness index, Stream power index, Sediment transport index, Topographic roughness index, distance from the river, LULC, geology, geomorphology, soil, rainfall, and elevation through a unified approach of an area.

Table 3 Pairwise comparison matrix

Parameters	Slope	TWI	SPI	STI	TRI	Distance from river	LULC	Geology	Geomorphology	Soil	Rainfall	Elevation
Slope	**1**	7	7	7	4	1	1/3	3	4	3	1/5	1/2
TWI	1/7	**1**	1	2	1/3	1/8	1/7	1/3	1/4	1/5	1/7	1/6
SPI	1/7	1	**1**	1	1/5	1/8	1/8	1/3	1/5	1/5	1/7	1/9
STI	1/7	1/2	1	**1**	1/5	1/8	1/8	1/3	1/4	1/6	1/7	1/9
TRI	1/4	3	5	5	**1**	1/7	1/4	1	1/2	1/5	1/5	1/6
Distance from river	1	8	8	8	7	**1**	3	4	4	3	2	1/2
LULC	3	7	8	8	4	1/3	**1**	4	2	2	1/3	1/5
Geology	1/3	3	3	3	1	1/4	1/4	**1**	1/2	1/3	1/5	1/5
Geomorphology	1/4	4	5	4	2	1/4	1/2	2	**1**	1/3	1/4	1/5
Soil	1/3	5	5	6	5	1/3	1/2	3	3	**1**	1/3	1/4
Rainfall	5	7	7	7	5	1/2	3	5	4	3	**1**	1/2
Elevation	2	6	9	9	6	2	5	5	5	4	2	**1**

(*Source* Calculated by the authors)

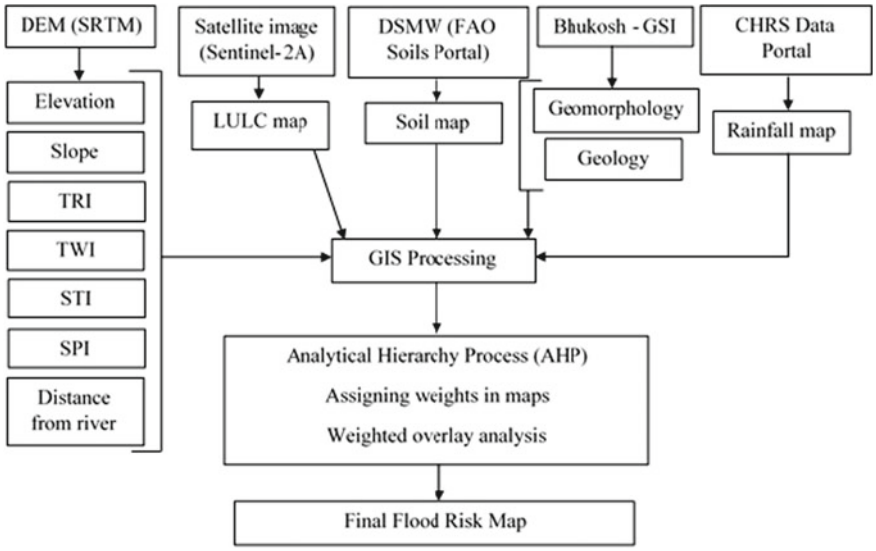

Fig. 2 Methodological flowchart for flood risk mapping

4.1 Slope Map

The slope is an essential geographical aspect that has a huge contribution to the occurrence of floods. During monsoon season, precipitated water quickly moves downslope from high slopes. If a high or steep slope covers an area, it has a high risk of making high flow velocity of runoff. Conversely, low or flat slopes are, therefore, more likely to experience waterlogging, which might result in excessive infiltration (Harshasimha and Bhatt 2023). This slope is categorized into three classes: 0–7.3, 7.3–18.6, 18.6–64.1. These classes covered 78.8%, 13.5%, and 7.7% of the total geographical area respectively (Fig. 3).

4.2 Topography Wetness Index (TWI)

A larger TWI value indicates greater flood risk (Fig. 4). In contrast, the steepest slope and least flood risk are indicated by a lower value (Gupta and Dixit 2021). The TWI value was classified as 2.9–8.4, 8.4–12.1, and 12.1–23.9. These classes occupied 59%, 25.1%, and 15.9% of the total area, respectively. In this, we have seen that the southern part denotes a lower value (topographic wetness value), but the remaining part of the study area comparatively denotes a high value, basically near the rivers. So, the study area is a highly flood-prone area except for some parts of the South.

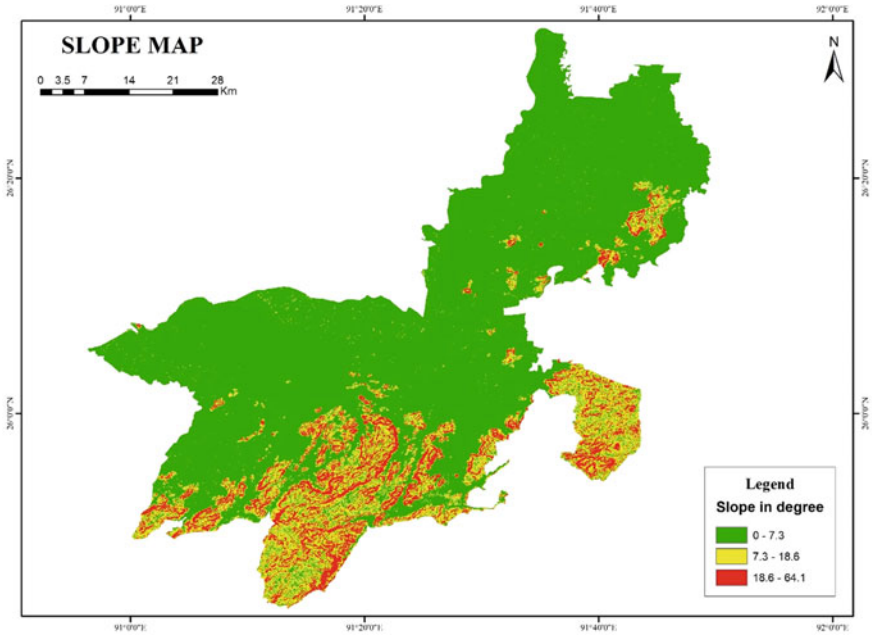

Fig. 3 Slope map of the study area

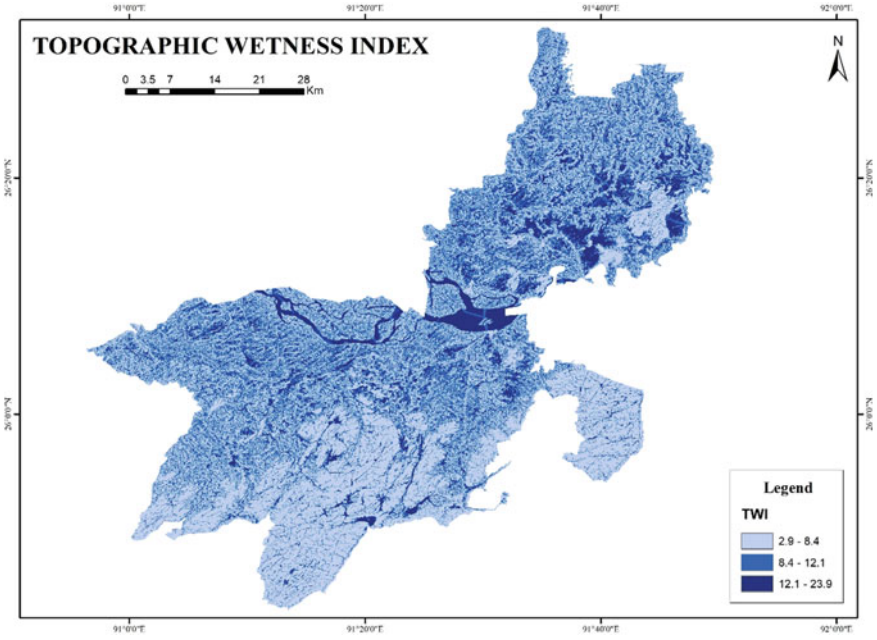

Fig. 4 Topographic wetness index map

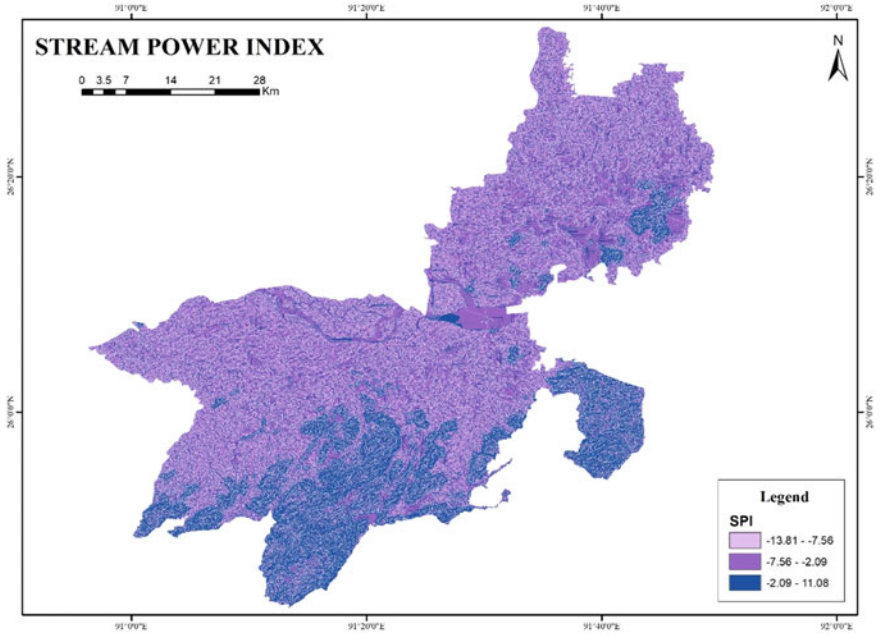

Fig. 5 Stream power index map

4.3 Stream Power Index (SPI)

SPI is crucial for calculating the erosive power caused by river flow or surface runoff (Das 2022). The SPI value ranges from −13.81 to 11.08 (Fig. 5). Low SPI levels correlate to wide alluvial flats, floodplains, and slowly subsiding terrain, while higher SPI values typically imply steep, straight areas (Kanwal et al. 2016).

4.4 Sediment Transport Index (STI)

The regional distribution of the sediment transport capability and accumulation is depicted by STI (Bannari et al. 2017). It is essential to flood risk assessment, river restoration, and environmental management. The STI value is categorized/classified into three classes: 0–10.6, 10.6–202.6, and 202.6–1359.6 (Fig. 6). Higher values signify the origin of sediment movement from steep inclines, while lower values show the location of sediment accumulation (Kulimushi et al. 2021).

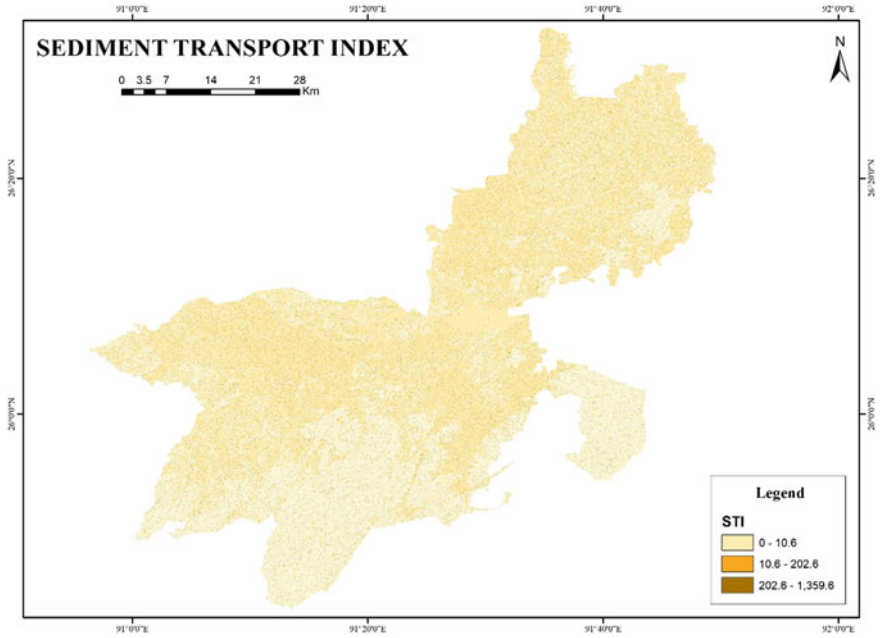

Fig. 6 Sediment transport index map

4.5 Topographic Roughness Index (TRI)

TRI is widely applicable for the analysis of flood mapping and monitoring. The Topographic Roughness Index is a measure used to quantify surface variety in the landscape (Stambaugh and Guyette 2008). The possibility of flood increasing is high with a lower TRI value (Amen et al. 2023). The TRI value of the study area was classified as 0.11–0.41, 0.41–0.57, and 0.57–0.88, and these classes covered 24.7%, 53.9%, and 21.4% of the total geographical area (Fig. 7).

4.6 Distance from the River

An area's distance from the river is crucial to flood risk modeling. The river's volume will exceed its drainage capacity during an overflow, and the water depth in the vicinity of the riverbed will quickly rise (Gupta and Dixit 2021). The surrounding area will experience waterlogging and a higher risk of flooding due to the flood inundation, not just the closest river (Gupta and Dixit 2021). People and agricultural land are closely situated near the banks of rivers/streams, and they are highly affected by floods. In this, we calculated the distance from the river and streams of the study

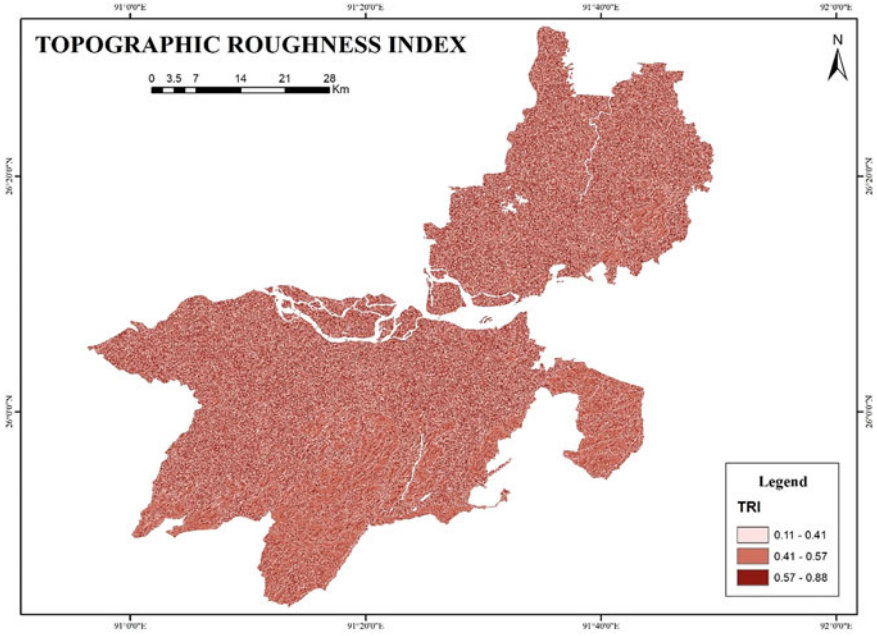

Fig. 7 Topographic roughness index map

area, and the distance up to greater than 2000 m (>2 km) is derived, which is classified into five classes of 500, 1000, 1500, 2000, >2000 m (Fig. 8).

4.7 Land Use and Land Cover (LULC Map)

The most crucial factors in determining the activities in the area and the types of LULC that are regularly impacted by flooding are land use and land cover (Das 2022). The link between several hydrological factors, such as runoff, infiltration, and rainfall absorption, is governed by LULC (Gupta and Dixit 2021). The LULC map was prepared using supervised classification involving the maximum likelihood classifier technique. Due to its direct influence on various hydrological factors such as surface runoff generation, infiltration, and rainfall abstraction, land use, and land cover have an impact on surface runoff as well as the movement of sediment, which in turn has an impact on the frequency of floods. Based on LULC classification, the entire area is divided into five major classes: agricultural land, built-up area, sandbar, vegetation and forest, and water body. Agricultural land covered 1226.25 km^2 (39.76%), followed by vegetation and forest 864.48 km^2 (28.03%), built-up area 532.93 km^2 (17.28%), sandbar 343.88 km^2 (11.15%), and water body 116.58 km^2 (3.78%) of the total geographical area (Fig. 9). Fluvial plains with high productivity

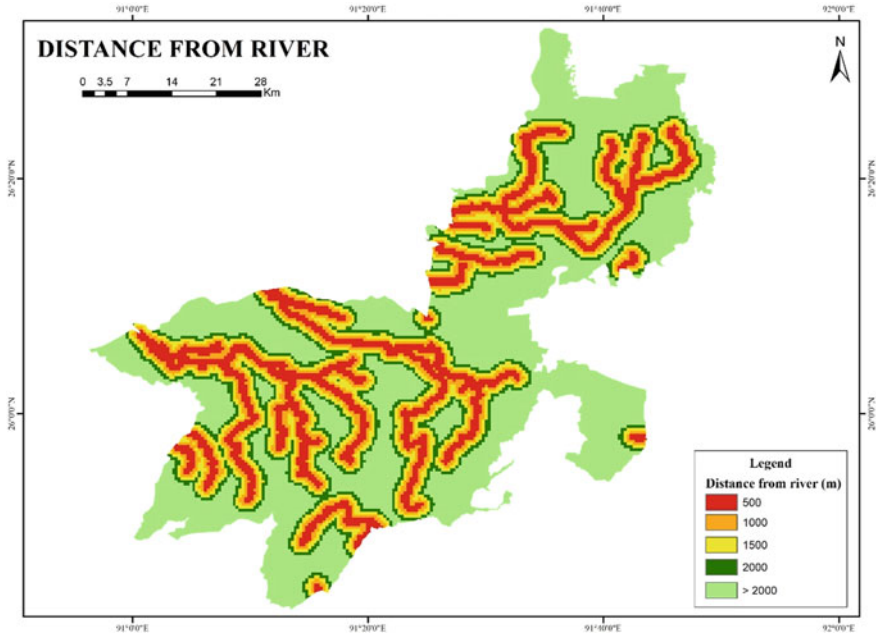

Fig. 8 Distance from the river map

are important for agricultural land, but these areas are most exposed to floods due to the increases of rainfall and the flow of water during monsoon season. The amount of surface runoff is reduced by the forest and plant cover (Hammam et al. 2022). Nevertheless, the impregnable surfaces of built-up regions increase surface runoff, which raises the possibility of flooding (Hammam et al. 2022).

4.8 Geology Map

The hydraulic characteristics of a region's bedrock are determined by its geology. Flood risk is reduced by the broken, highly porous, and permeable bedrock, which increases the rate at which precipitation infiltrates (Gupta and Dixit 2021). There are three categories on the study area's geological map. (1) Undiff. Fluvial/Aeolian/Coasta and Glacial Sediments (Quaternary), (2) Assam–Meghalaya Gneissic Complex (Proterozoic), and (3) Kyrdem, Nongpoh, Mylliem Granite, S. Khasi Batholiths and Equivalent Granites (Neoproterozoic–Early Palaeozoic) and these groups covered almost 73.14%, 20.91%, and 5.95% of the total geographical area respectively (Fig. 10).

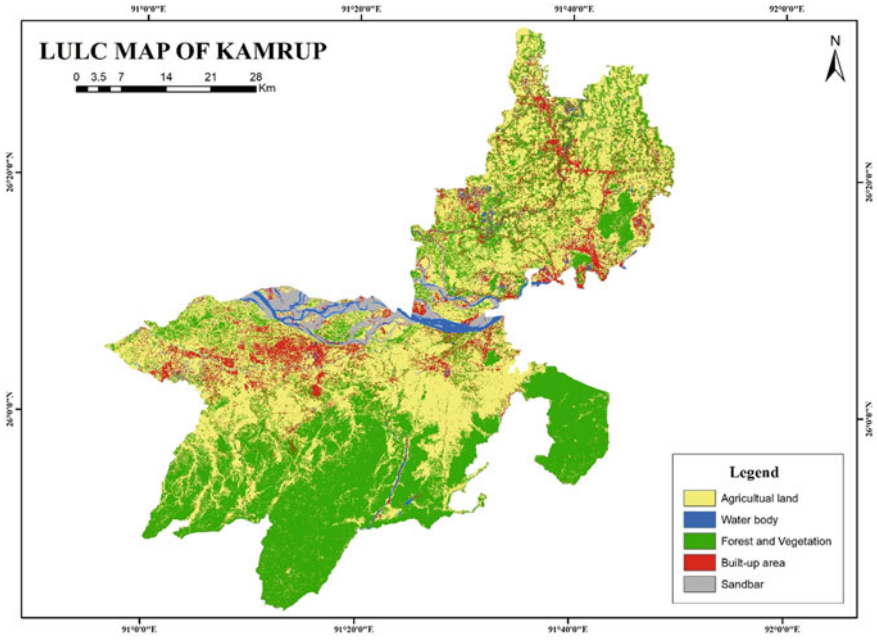

Fig. 9 LULC map of study area

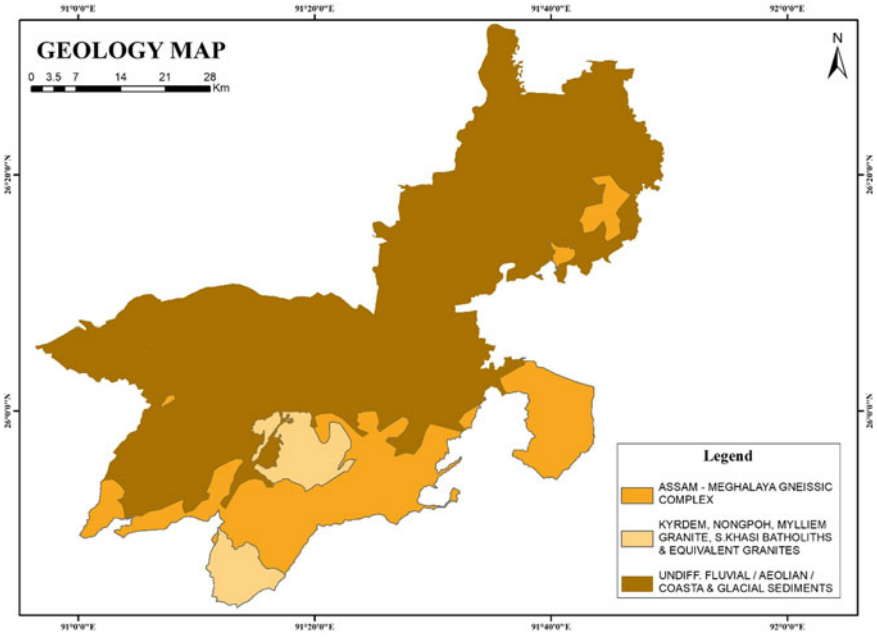

Fig. 10 Geological map

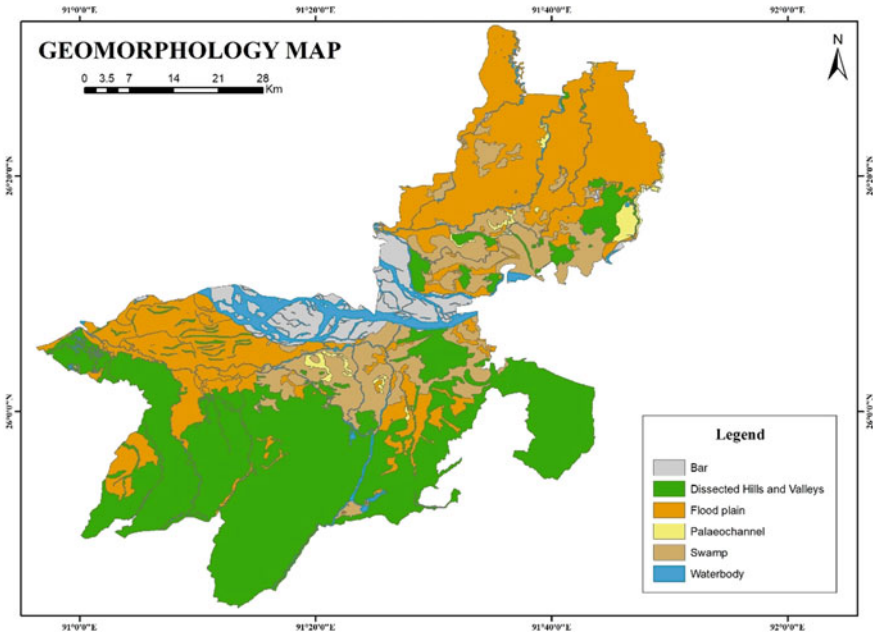

Fig. 11 Geomorphological map

4.9 Geomorphology Map

Geomorphological characteristics are the salient features for flood formation in an area. Floods give rise to erosional and depositional landforms (Gupta and Dixit 2021). The study area is categorized into six major geomorphology groups. (1) Dissected Hills and Valleys, (2) Flood Plain, (3) Swamp, (4) Water bodies, (5) Bar, and (6) Palaeochannel, and these groups occupied/covered almost 42.69%, 32.66%, 12.65%, 5.71%, 5.01%, and 1.28% of the total geographical area respectively (Fig. 11).

4.10 Soil Map

Given that the prevailing soil texture substantially influences the regional internal drainage system, surface runoff, and moisture contents, soil texture is an important predictor of flood hazards (Gupta and Dixit 2021). One of the most significant contributing variables to the generation of rainfall and runoff is the different kinds of soil. The study area is classified into two soil classes/groups. One is Ao (Orthic Acrisols) or sandy clay loam, and another is Nd (Dystric Nitosols) or loam (Fig. 12). Ao and Nd soil groups covered almost 81.55% and 18.45% of the total area respectively.

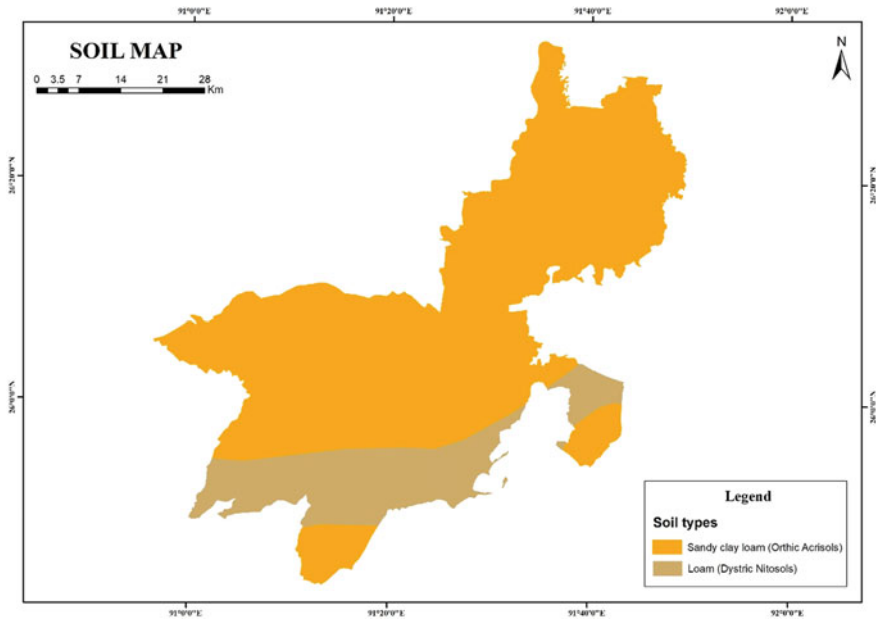

Fig. 12 Soil map of study area

4.11 Rainfall Distribution Map

The primary determinant of flood frequency during the monsoon season is precipitation. Floods could result from a lot of rain in a short period. Over 18 years, from 2003 to 2020, data on annual rainfall was gathered from eight areas within the study area. The areas are—Hajo, Rangia, Chaygaon, Bezera, Boko, Goroimari, Sualkuchi, and Rani. Each station's latitude and longitude (X, Y data) were gathered in order to interpolate the study area's total rainfall. The maximum average rainfall was recorded in the Rani area (1748 mm), while Rangia, Bezera, Hajo, and Sualkuchi (1099, 1109, 1163, and 1176 mm) areas recorded minimum average rainfall for 18 years (Fig. 13). The rainfall data is categorized into five classes, from very low to very high. The average rainfall amount increases from northeast to southwest in the study area.

4.12 Elevation Map

The most crucial element in defining flood hazard modeling and monitoring is elevation. The relationship between flooding and height is inverse (Amen et al. 2023). If it is high elevation, then the vulnerability of floods is low, inversely if it is low elevation, then it has a high risk of flood. We found that most of the areas were low elevated. The study displays the diversity in elevation in five groups as 20–241.4, 241.4–462.8,

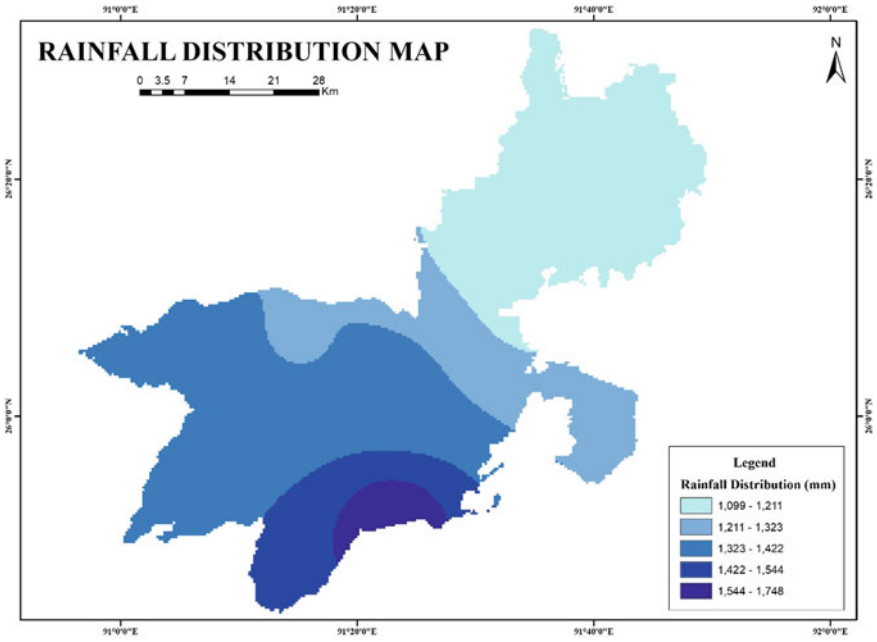

Fig. 13 Rainfall distribution map

462.8–684.2, 684.2–905.6, and 905.6–1127 range (Fig. 14). These classes occupied 88%, 8.25%, 2.05%, 1.4%, and 0.3% of the total area respectively.

4.13 Flood Risk Map

In order to identify the flood risk zones in the research area, the AHP approach and the weighted overlay method were integrated to create the final flood risk map. The flood risk zones were determined by giving weights to the various factors on maps and selecting the appropriate ranking for them. Slope, TWI, SPI, STI, TRI, distance from the river, LULC, geology, geomorphology, soil, rainfall, elevation, and 10.7, 1.8, 1.4, 3.7, 16.2, 10.7, 3.5, 4.9, 7.7, 16.2, and 21.3% were the assigned weights for each of the thematic layers (Table 4). The highest weight is assigned in the elevation map (21.3%), and the lowest weight is assigned in the STI map (1.4%). The lowest rank of assigning weight bearing is less important, whereas the highest rank of assigning weight bearing is more important for flood risk mapping and monitoring. The output value of consistency ratio (CR) is 0.0931 (9.31%) < 0.1 (10%).

There were five categories on the final flood risk map: very low, low, moderate, high, and very high. The areas that these classes occupied were 0.01 and 31.46, 1770.21, 62.44, and 1220.02 km^2 (Table 5). Of the entire geographical area, the

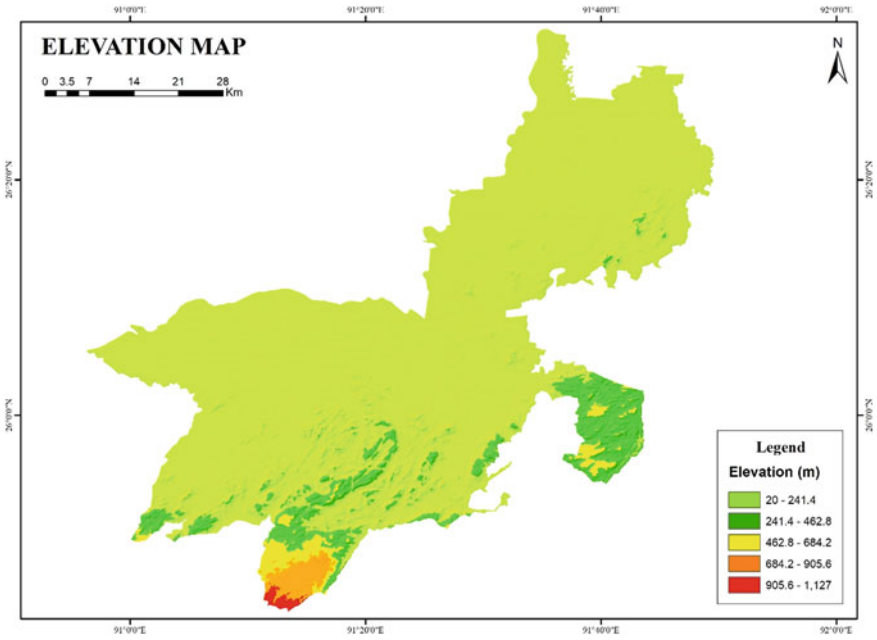

Fig. 14 Elevation map

extremely low-risk zone only makes up 0.01 km^2, whereas the high-risk zone comprises the largest area at 1770.21 km^2 (57.40%) (Fig. 15). Flood risk zones classified as high or extremely high-risk originate from regions with low elevation (less than 241.4 m), gentle slope (less than 7.3°), and close proximity to a river (less than 2000 m). The flat slope and proximity to the river allow flood water to stay for a longer duration and inundate the low-lying areas. Also, these zones reflected higher values of TWI and SPI and lower values of STI and TRI area/region, which attribute to their occupancy in these zones. From the LULC map, it is distinctive that these zones are dominantly human-induced landscapes, including built-up areas and agricultural land. Due to intensive anthropogenic activities, flood risk is also highest in these areas. Even though these zones do not receive a lot of rainfall, water from nearby hills and uplands rushes towards these low-lying areas, exacerbating the study area's flood risk scenario. The picture becomes more prominent during the monsoon season, which puts the lives of people and allied activities at stake. The study area's moderate flood risk zone included the northern portion as well as the extremely elevated sections in the south and southeast. A little over 1220.02 km^2 of the research area is at moderate risk of flooding.

The GIS yielded risk map was validated with a primary field visit by randomly selecting villages from each block (Fig. 16) (Table 6). The result reveals that blocks that lie in their respective zones as per Table 6 corroborate with field visits

Table 4 Sub criteria of each parameter and their weights

Flood causative criterion	Unit	Class	Rank (very high = 5, very low = 1)	Category/ intensity	Weight (%)
Slope	°	0–7.3	5	Very high	11.1
		7.3–18.6	4	High	
		18.6–64.1	3	Moderate	
TWI	Level	2.9–8.4	3	Moderate	1.8
		8.4–12.1	4	High	
		12.1–23.9	5	Very high	
SPI	Level	−13.81 to −7.56	3	Moderate	1.5
		−7.56 to −2.09	4	High	
		−2.09–11.08	5	Very high	
STI	Level	0–10.6	5	Very high	1.4
		10.6–202.6	4	High	
		202.6–1359.6	3	Moderate	
TRI	Level	0.11–0.41	5	Very high	3.7
		0.41–0.57	4	High	
		0.57–0.88	3	Moderate	
Distance from river	m	500	5	Very high	16.2
		1000	4	High	
		1500	3	Moderate	
		2000	2	Low	
		>2000	1	Very low	
LULC	Class	Agricultural land	5	Very high	10.7
		Water body	5	Very high	
		Sandbar	5	Very high	
		Built-up area	4	High	
		Vegetation and forest	3	Moderate	
Geology	Class	Undiff. Fluvial/Aeolian/ Coasta and glacial sediments	5	Very high	3.5
		Assam–Meghalaya gneissic complex	2	Low	
		Kyrdem, Nongpoh, Mylliem Granite, S. Khasi Batholiths and equivalent granites	1	Very low	
Geomorphology	Class	Bar	5	Very high	4.9
		Flood plain	5	Very high	
		Palaeochannel	5	Very high	

(continued)

Table 4 (continued)

Flood causative criterion	Unit	Class	Rank (very high = 5, very low = 1)	Category/ intensity	Weight (%)
		Water body	5	Very high	
		Swamp	4	High	
		Dissected hills and valleys	3	Moderate	
Soil	Class	Ao	5	Very high	7.7
		Nd	3	Moderate	
Rainfall	mm/ year	1099–1211	1	Very low	16.2
		1211–1323	2	Low	
		1323–1422	3	Moderate	
		1422–1544	4	High	
		1544–1748	5	Very high	
Elevation	m	20–241.4	5	Very high	21.3
		241.4–462.8	4	High	
		462.8–684.2	3	Moderate	
		684.2–905.6	2	Low	
		905.6–1127	1	Very low	

(*Source* Calculated by the authors)

Table 5 Demarcation of flood potential zones

Flood potential zones	Area (in km^2)	Area (in %)
Very low	0.01	0.00
Low	31.46	1.02
Moderate	1220.02	39.56
High	1770.21	57.40
Very high	62.44	2.02
Total	3084.14	100

(*Source* Calculated by the authors)

and data reported by (District Agricultural Development Strategy of KAMRUP—District, n.d.). Blocks including Goroimari, Hajo, Boko, Chamaria, Chayani Barduar, and Chaygaon are located in areas with a very high to high risk of flooding. As reported by (District Agricultural Development Strategy of KAMRUP—District, n.d.), these blocks are also highly vulnerable to soil erosion and sand deposition. These phenomena have been attributed to a high frequency of floods as reported in (District Agricultural Development Strategy of KAMRUP—District, n.d.). Thus, it can be inferred that GIS-generated output very well represents the ground reality concerning flood risk and monitoring.

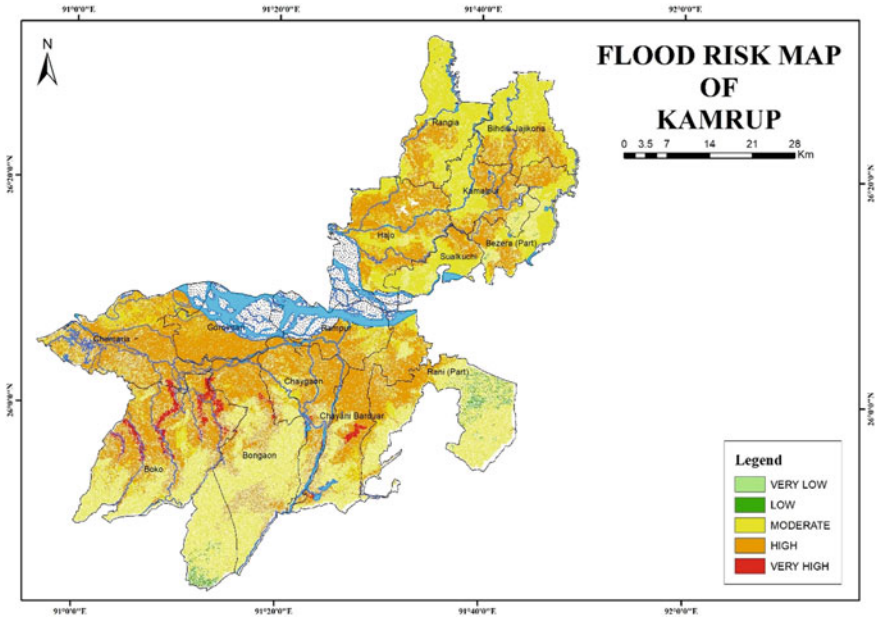

Fig. 15 Flood risk map of Kamrup

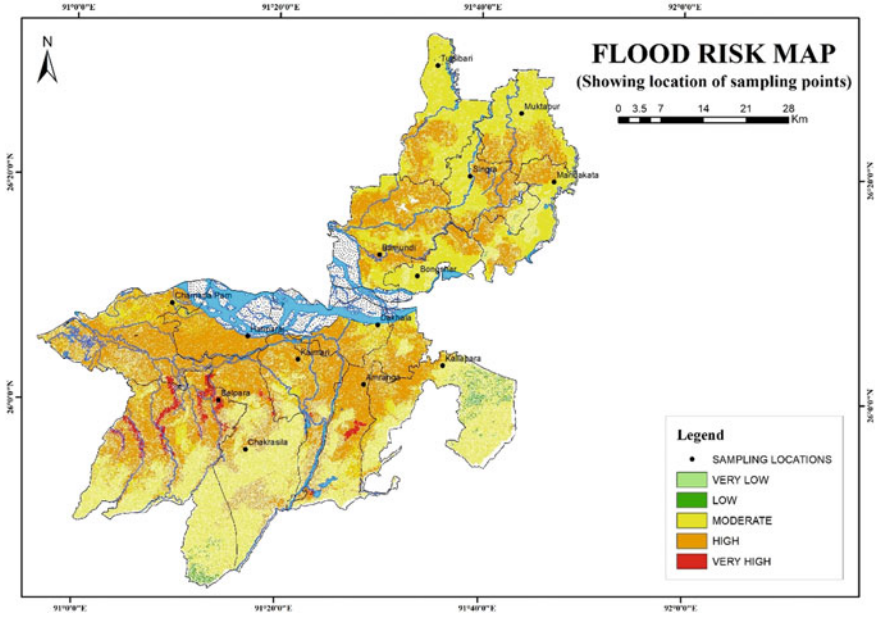

Fig. 16 Flood risk map (Showing location of sampling points)

Table 6 Location for validation of GIS output

Block	Village	Latitude (°N)	Longitude (°E)	Flood risk (as per GIS output)
Bezera	Mandakata	26.32853	91.78622	Moderate
Bihdia-Jajikona	Muktapur	26.42964	91.73164	Moderate
Boko	Belpara	25.99946	91.23867	Very high
Bongaon	Chakrasila	25.92718	91.28398	Moderate
Chamaria	Chamaria Pam	26.14321	91.16078	High
Chayani Barduar	Amranga	26.02545	91.47666	High
Chaygaon	Kaimari	26.06159	91.36823	High
Goroimari	Hatipara	26.09503	91.28546	High
Hajo	Bamundi	26.21808	91.50021	High
Kamalpur	Singra	26.33589	91.64816	Moderate
Rampur	Dakhala	26.11388	91.49876	Moderate
Rangia	Tulsibari	26.49946	91.59325	Moderate
Rani	Kallapara	26.05479	91.60616	Moderate
Sualkuchi	Bongshar	26.18694	91.56311	Moderate

(*Source* Calculated by the authors)

5 Conclusion

In conclusion, this study uses cutting-edge geospatial approaches to tackle the important problem of flood risk in the Kamrup area of Assam. The main goal was to map and monitor areas affected by flooding, emphasizing creating an extensive map of flood risk that can guide mitigation efforts and emergency readiness.

The synthesis of various thematic layers, such as slope, Topography Wetness Index (TWI), Stream Power Index (SPI), Sediment Transport Index (STI), Topographic Roughness Index (TRI), distance from the river, land use/land cover (LULC), geology, geomorphology, soil, rainfall, and elevation, was made possible by the combination of the Analytic Hierarchy Process (AHP) technique and the weighted overlay method. Based on a methodical ranking approach, weights were assigned to these layers to represent their respective relevance in flood risk assessment. With the highest weight assigned (21.3%), the elevation layer stood out as the most significant, highlighting its critical role in controlling flood risk. The resulting flood risk map provides a detailed picture of the study's susceptibility landscape, with areas categorized as very low, low, moderate, high, and very high. The high potential zone, covering an extensive area of 57.40%, indicates regions with the highest susceptibility to flooding. Conversely, the very low potential zone, occupying a minimal area of 0.01 km^2, represents areas with the lowest risk. These classifications were derived from key parameters, including low elevation, flat slope, proximity to the river, higher values of TWI and SPI, and lower values of STI and TRI.

The practical significance of this research extends beyond academic realms. Identifying high-risk zones in built-up and agricultural areas emphasizes the urgent need for targeted disaster management strategies. In order to protect people and property during the monsoon season, the study offers municipal authorities, urban planners, and legislators a useful tool for putting pre-emptive measures into place, such as early warning systems, land-use planning, and infrastructure development.

In conclusion, the research contributes to the academic understanding of flood risk assessment and serves as a practical guide for informed decision-making. This study establishes the foundation for resilient, sustainable, and adaptive solutions to lessen the impact of floods on vulnerable populations by identifying and measuring flood risk. The integration of geospatial techniques and AHP methodology showcases a replicable approach that can be adapted for similar studies globally, offering a significant contribution to disaster risk management.

References

Amen ARM, Mustafa A, Kareem DA, Hameed HM, Mirza AA, Szydłowski M, Saleem BKM (2023) Mapping of flood-prone areas utilizing GIS techniques and remote sensing: a case study of Duhok, Kurdistan region of Iraq. Remote Sens 15(4):1102. https://doi.org/10.3390/rs15041102

Anusha N (2021) Flood detection and mapping from multitemporal sentinel 1a synthetic aperture radar imagery using automated flood delineation technique. Doctoral dissertation. http://hdl.handle.net/10603/352329

Bachri S, Sumarmi, Yudha Irawan L, Utaya S, Dwitri Nurdiansyah F, Erfika Nurjanah A, Wahyu Ning Tyas L, Amri Adillah A, Setia Purnama D (2019) Landslide susceptibility mapping (LSM) in Kelud volcano using spatial multi-criteria evaluation. IOP Conf Ser Earth Environ Sci 273(1):012014. https://doi.org/10.1088/1755-1315/273/1/012014

Bannari A, Ghadeer A, El-Battay A, Hameed NA, Rouai M (2017) Detection of areas associated with flash floods and erosion caused by rainfall storms using topographic attributes, hydrologic indices, and GIS. Glob Changes Natl Disaster Manag Geo-inf Technol 155–174. https://www.researchgate.net/publication/315619883

Bhatt C, Rao G (2014) Ganga floods of 2010 in Uttar Pradesh, North India: a perspective analysis using satellite remote sensing data. Geomat Nat Haz Risk 7(2):747–763. https://doi.org/10.1080/19475705.2014.949877

Choudhury S, Garg B (2021) Groundwater potential mapping of East Guwahati: a geospatial study. In: Sustainable approach to resource management for social development. Assam Book Hive, pp 45–59

Das B (2022) Flood hazard mapping and road network vulnerability analysis of Kamrup and Kamrup metropolitan districts: case study of Assam flood 2019. Int J Sci Res (IJSR) 11(5):314–324. https://www.ijsr.net/archive/v11i5/SR22501092926.pdf

District Agricultural Development Strategy of KAMRUP—District (n.d.) Agricultural technology management agency (ATMA), Kamrup

District Profile (n.d.) Kamrup District | Government of Assam, India. https://kamrup.assam.gov.in/about-us/district-profile

Flood and Erosion Problems (2023, September 12) Water Resources | Government of Assam, India. https://waterresources.assam.gov.in/portlets/flood-erosion-problems

Floods (n.d.) NDMA, GoI. https://ndma.gov.in/Natural-Hazards/Floods

Gupta L, Dixit J (2021) A GIS-based flood risk mapping of Assam, India, using the MCDA-AHP approach at the regional and administrative level. https://doi.org/10.21203/rs.3.rs-1015728/v1

Hammam N, Abdulwahab K, Mohamed AS (2022) Flood monitoring using remote sensing and GIS techniques: a case study of Kampala district, Uganda. J Multidiscip Eng Sci Technol (JMEST) 09(10):15540–155545. https://www.researchgate.net/publication/364965837

Harshasimha AC, Bhatt CM (2023) Flood vulnerability mapping using MaxEnt machine learning and analytical hierarchy process (AHP) of Kamrup Metropolitan district, Assam. ECWS-7 2023. https://doi.org/10.3390/ecws-7-14301

Hazarika S (2015) Flood in Kamrup Metropolitan district Assam vulnerability patterns and management strategies. Doctoral dissertation. http://hdl.handle.net/10603/114338

Kanwal S, Atif S, Shafiq M (2016) GIS based landslide susceptibility mapping of northern areas of Pakistan, a case study of Shigar and Shyok Basins. Geomat Natl Hazards Risk 8(2):348–366. https://www.researchgate.net/publication/306526329

Kulimushi LC, Bashagaluke JB, Choudhari P, Masroor M, Sajjad H (2021) Novel combination of analytical hierarchy process and weighted sum analysis for watersheds prioritization. A study of Ulindi catchment, Congo River Basin. Geocarto Int 37(25):8456–8494. https://www.researchgate.net/publication/355947701

Lahkar B (2017) Education occupation and health status among the scheduled cast population in Kamrup district Assam. Doctoral dissertation. http://hdl.handle.net/10603/223380

Manual for Data Collection in Census of Water Bodies (n.d.) Directorate of economics and statistics, Odisha, Bhubaneswar

Rahimi S, Malakooti H, Aliakbari Bidokhti A (2023) Investigation of the chemical nature of precipitation and source apportionment of its constituents in Tehran metropolis, Iran. Environ Res 225:115587. https://doi.org/10.1016/j.envres.2023.115587

Reddy GP, Singh SK (2018) Geospatial technologies in land resources mapping, monitoring and management. Springer

Rehman S, Sahana M, Hong H, Sajjad H, Ahmed BB (2019) A systematic review on approaches and methods used for flood vulnerability assessment: framework for future research. Nat Hazards 96(2):975–998. https://doi.org/10.1007/s11069-018-03567-z

Saaty TL (2008) Decision making with the analytic hierarchy process. Int J Serv Sci 1(1):83–98. https://doi.org/10.1504/IJSSCI.2008.017590

Sharma V, Singh D (n.d.) NTA UGC NET/JRF/SET PAPER-2 Geography. Arihant Publications (Inida) Limited

Sonowal K, Choudhury S (2023) Geospatial study to assess Asian elephant habitat suitability in Rani-Garbhanga reserve forest. In: ANWESHAN: a collection of articles, 1st ed. J S Publications, pp 222–235

Stambaugh MC, Guyette RP (2008) Predicting spatio-temporal variability in fire return intervals using a topographic roughness index. For Ecol Manag 254(3):463–473. https://doi.org/10.1016/j.foreco.2007.08.029

Tam TH, Ibrahim AL, Abd Rahman MZ, Zulkifli M (2013) Flood risk mapping using geospatial technologies and hydraulic model